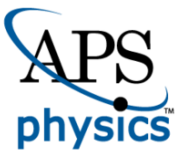

Significance of electrically induced shear stress in drainage of thin aqueous films

Christiaan Ketelaar and Vladimir S. Ajaev

Phys. Rev. E **91**, 052403 — Published 19 May 2015

DOI: 10.1103/PhysRevE.91.052403

The significance of electrically induced shear stress in drainage of thin aqueous films

Christiaan Ketelaar
Department of Mathematical Sciences, University of Delaware, Newark, DE 19716, USA

Vladimir S. Ajaev
Department of Mathematics, Southern Methodist University, Dallas TX 75275, USA and Institute of Power Engineering, Tomsk Polytechnic University, Tomsk 634050, Russia

We develop a novel model of drainage of microscale thin aqueous film separating a gas bubble and a solid wall. In contrast to previous studies, the electrostatic effects are accounted for not only in the normal but also in the shear stress balance at the liquid-gas interface. We show that the action of the tangential component of the electric field leads to potentially strong spatially variable shear stress at the deforming charged interface. This previously overlooked effect turns out to be essential for correctly estimating the long-time drainage rates. Comparison of time-dependent fluid interface shapes predicted by our model with the experimental data is discussed.

I. INTRODUCTION

The problem of drainage of a thin aqueous film is important for a number of applications such as flotation, lab-on-a-chip devices, and microscale two-phase cooling systems. Experimental studies of drainage usually involve a droplet or bubble formed at the top of a capillary and pressed against a solid wall [1–4]. Fluid interface evolution is then recorded using interferometry. Typical results indicate that the interface forms a dimple, although more complicated rippled deformations have been recorded and explained recently [5, 6]. The interface deformation provides the capillary pressure gradient needed to drive the flow in the viscous film between the deforming interface and the wall. The flow in the film is usually described using lubrication-type models, valid when the film thickness is much smaller than other relevant geometric length scales [7, 8]

Mathematical models of viscous drainage typically incorporate the physical effects of both surface tension and disjoining pressure. The latter refers to additional terms in the stress tensor in the liquid film arising when the film thickness is on micro- and nanoscale due to effects such as London-van der Waals dispersion forces and electrostatic repulsion/attraction between electrically charged interfaces [9, 10]. The contribution from the dispersion forces is usually assumed to be inversely proportional to the cube of local thickness of the draining film, while the electrostatic component of disjoining pressure is described based on theories of interaction of electrical double layers formed near charged interfaces in aqueous solutions. Mathematical models have been remarkably successful in explaining experimental data on drainage of films separating mercury droplets and mica substrate [8, 11]. However, when applied to the case of an aqueous film between a gas bubble and a solid surface, the agreement between theory and experiments is rather poor when the standard hydrodynamic boundary conditions are used, as reported by Manica & Chan [12]. These authors also point out that good agreement can be achieved when the no-slip condition is forced at the deforming fluid interface. While there is substantial experimental evidence for finite rather than infinite slip length at the interfaces between aqueous solutions and air [13], most likely due to the contamination by surfactants, the assumption of complete interface immobilization without added surfactant (required to achieve agreement with experimental data in [12]) is rather unusual for liquid-gas interfaces.

In the present study, we explore the possibility of another, previously overlooked, factor in the drainage process, by revisiting the basic assumptions of the disjoining pressure approach. The latter provides a convenient method for incorporating the electrostatic effects into the normal stress balance at the fluid interface but completely neglects these effects in the shear stress balance. We show that electrostatic contributions to both stress balances are important in a thin aqueous layer separating a gas bubble from a solid wall and develop a model which accounts for these contributions. The physical mechanism of the additional term in the shear stress balance is simply the action of the tangential component of the electric field on the interfacial charges.

II. FORMULATION

Consider a gas bubble protruding from a circular tube surrounded by viscous liquid which is a 1:1 symmetric aqueous electrolyte. The bubble is pressed against a flat solid wall, resulting in drainage of the liquid layer separating the bubble from the wall, as sketched in Fig. 1. The radius of curvature of the bubble away from the wall is R_0 and the configuration is assumed axisymmetric. The wall is at a constant electric potential denoted by ψ_w, while the liquid-gas interface has a constant electric charge density q_i. We note that in contrast to the case of a mercury droplet pressed against the wall, there is no physical reason to expect the potential at the deforming liquid-gas interface to remain constant. Interfacial charges at the film boundaries are screened by the layers

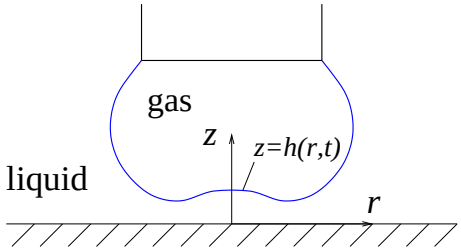

FIG. 1. (Color online) Sketch of an axisymmetric bubble pressed against a solid wall, also showing nondimensional cylindrical coordinates.

of charge of characteristic thickness equal to the Debye length,

$$\lambda_D = \sqrt{\frac{\varepsilon k_B T}{2 n_0 e^2}}, \tag{1}$$

where ε is the dielectric permittivity, k_B is the Boltzmann constant, T is the temperature, n_0 is the bulk ion concentration in the electrolyte, e is the elementary charge. The dynamics of the film is governed by the interplay of surface tension and the electrostatic interaction between the interfacial double layers; the effects of London-van der Waals dispersion forces are assumed negligible, as is often the case in experimental studies [2, 4].

The dimensional governing equations couple together the pressure p^*, viscous flow velocity $\mathbf{u}^*$, and electric potential ψ^* in the liquid as follows,

$$\nabla p^* = \mu \nabla^2 \mathbf{u}^* - \rho_E \nabla \psi^*, \tag{2}$$

$$\nabla \cdot \mathbf{u}^* = 0, \tag{3}$$

$$\nabla^2 \psi^* = \lambda_D^{-2} \sinh \psi^*. \tag{4}$$

Here μ is the dynamic viscosity of the liquid, ρ_E is the electrical charge density; both the Reynolds number and the Bond number are assumed to be small, as appropriate for many microscale applications.

The time-dependent interface position is represented in cylindrical coordinates by a function $z^* = h^*(r^*, t^*)$, where t^* is time and $z^* = 0$ corresponds to the solid wall. The interfacial normal and shear stress balances are then written in terms of the hydrodynamic part of the stress tensor $\mathbf{T}^f$ of the liquid as

$$\mathbf{n} \cdot \mathbf{T}^f \cdot \mathbf{n} + p_0^* + \frac{q_i^2}{2\varepsilon} - \frac{1}{2}\varepsilon (\nabla \psi^* \cdot \mathbf{t})^2 = \sigma \left(\frac{h^*_{r^* r^*}}{(1 + h^{*2}_{r^*})^{3/2}} + \frac{h^*_{r^*}}{r^* (1 + h^{*2}_{r^*})^{1/2}} \right), \tag{5}$$

$$\mathbf{t} \cdot \mathbf{T}^f \cdot \mathbf{n} + q_i (\nabla \psi^* \cdot \mathbf{t}) = 0, \tag{6}$$

where $\mathbf{n}$ and $\mathbf{t}$ are the unit normal and tangential vectors to the interface, respectively, p_0^* is the pressure in the gas inside the bubble, σ is the surface tension. Viscous stresses in the gas phase are neglected in our formulation. The electrostatic contributions to the above interfacial stress balances are derived from the general expressions for the Maxwell stress tensors, as discussed e.g. in Saville [14], with the assumption of the dielectric permittivity of liquid being much larger than that of the gas phase. At the interface, we also apply the standard kinematic boundary condition for the flow and the following condition for the electric potential,

$$\nabla \psi^* \cdot \mathbf{n} = \frac{q_i}{\varepsilon}. \tag{7}$$

At the solid wall, $\mathbf{u}^* = 0$ and $\psi^* = \psi_w$.

In order to apply the lubrication-type approach [15–17], we define nondimensional cylindrical coordinates and time according to

$$r = \frac{r^*}{\mathrm{Ca}^{1/3} R_0}, \quad z = \frac{z^*}{\mathrm{Ca}^{2/3} R_0}, \quad t = \frac{U t^*}{\mathrm{Ca}^{1/3} R_0}. \tag{8}$$

Here we use the capillary number $\mathrm{Ca} = \mu U/\sigma \ll 1$ and choose the velocity scale U based on balance of the electrostatic and surface tension forces in equation (5), leading to

$$U = \frac{\sigma^{1/4}}{\mu} \left(\frac{\varepsilon \bar{\psi}^2}{R_0} \right)^{3/4}, \tag{9}$$

where $\bar{\psi} = k_B T/e$ is the characteristic electric potential.

The nondimensional electric potential ψ (scaled by $\bar{\psi}$) satisfies the nonlinear Poisson-Boltzmann equation

$$\psi_{zz} = \kappa^2 \sinh \psi, \tag{10}$$

where κ is the ratio of the vertical length scale and the Debye length. The scaled boundary conditions for this equation are those of constant potential $\hat{\psi} = \psi_w/\bar{\psi}$ at the wall ($z = 0$) and constant charge density $\tilde{q} = q_i \lambda_D/\varepsilon\bar{\psi}$ at the deforming interface, $z = h(r, t)$. The values of the gas-liquid interfacial potentials and charge densities are still a matter of controversy, as discussed e.g. in Pushkarova & Horn [4]; we used $\tilde{q} = -0.5$ in all simulations, but also verified that the conclusions of the present paper remain valid for $\tilde{q} = -1$ and $\tilde{q} = -1.5$.

The nondimensional versions of equations (5) and (6) in the limit of small capillary numbers are

$$p - \frac{1}{2}\psi_z^2 = -h_{rr} - r^{-1} h_r, \tag{11}$$

$$u_z + \psi_z (\psi_r + h_r \psi_z) = 0. \tag{12}$$

Here p is the pressure difference between liquid and gas scaled by σ/R_0, u is the radial velocity scaled by U. Note that equation (12) incorporates the electrostatic contribution to the shear stress at the liquid-gas interface, neglected in all previous studies of drainage despite the fact

that this contribution does not vanish in the asymptotic limit of small capillary numbers.

Following the standard lubrication-type approach [17], the system of governing equations is reduced to a nonlinear equation for the scaled film thickness,

$$h_t + (3r)^{-1}\left[rh^3\left(h_{rr} + r^{-1}h_r - \kappa^2\cosh\tilde{\psi}\right)_r\right]_r$$

$$-\kappa\tilde{q}(2r)^{-1}\left[rh^2\tilde{\psi}_h h_r\right]_r = 0, \qquad (13)$$

where $\tilde{\psi}$ is the scaled electric potential at the interface found from the numerical solution of the full Poisson-Boltzmann equation (10) with the boundary conditions specified above. In contrast to most previous studies of drainage, we do not rely on approximate expressions for the electrostatic potential in the film. Other than that, our numerical procedure is essentially the same as in Ajaev et al. [6]. In particular, we apply the symmetry conditions at $r = 0$ and use local Taylor expansions of derivatives in powers of r to eliminate singular terms prior to discretization. We fix the value of curvature at a position $r = L$ with the value of L chosen sufficiently large, corresponding to undeformed meniscus region away from the substrate. The initial profile is that of constant curvature,

$$h(r,0) = h_0 + \frac{1}{2}r^2, \qquad (14)$$

with h_0 corresponding to the dimensional value of 40 μm of initial separation between the interface and the solid wall. Starting at $t = 0$, the value of $h(L)$ is decreased over a short time interval Δt at a speed corresponding to 2.75 mm s^{-1} to simulate the experimental procedure, as discussed in Manica & Chan [12].

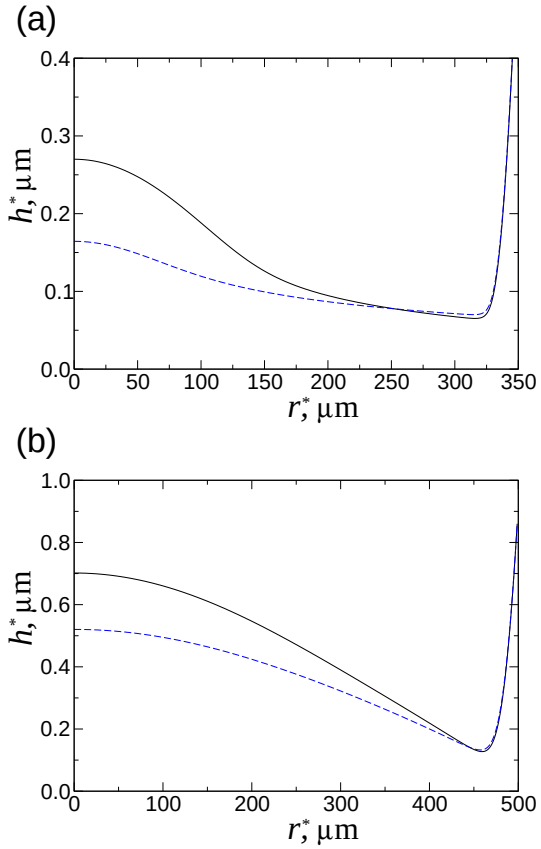

FIG. 2. (Color online) Comparison of interface shapes obtained with the shear stress variations included into the model (black solid lines) and neglected (blue dashed lines) for two parameter sets based on experimental studies of drainage [2]: (a) 0.25 mM salt solution, $\kappa = 4.29$, $\hat{\psi} = -5.06$, $t^* = 250$ s; (b) pure water, $\kappa = 0.384$, $\hat{\psi} = -5.76$, $t^* = 50$ s.

III. RESULTS AND DISCUSSION

A. Effect of electrically induced shear stress

Let us start by conducting the simulations of interface evolution for the parameter values corresponding to the drainage experiment of Hewitt et al. [2] with NaCl solution of concentration 0.25 mM. Based on the Debye length $\lambda_D = 19.23$ nm and the measured wall potential of $\psi_w = -130$ mV, we use $\kappa = 4.29$ and $\hat{\psi} = -5.06$ in our nondimensional formulation. The scaled computational domain size corresponds to $L^* = 400$ μm. We choose $\Delta t = 0.221$ to achieve the best fit to the experimental data. Dimensional numerical interface shape at $t^* = 250$ is shown in Fig. 2(a), black solid line. To illustrate the significance of the electrically induced tangential component of the interfacial stress, we also ran the simulation with the corresponding term in the evolution equation set to zero. The resulting interface shape, shown by the dashed blue line in Fig. 2 (a), is clearly different from the predictions of the full simulation, especially in the value of the film thickness at the axis of symmetry. The differences are seen for all values of time, but are most significant for long-time drainage.

Experimental studies of drainage of aqueous solutions have been conducted over a wide range of solute concentrations, so it is natural to ask how the predictions of the model depend on concentration. In the framework of our model, the changes in concentration mostly affect the nondimensional parameter κ, so we conducted simulations over a range of values of this parameter. We observed that at smaller κ the electrical shear stress contribution manifests itself earlier in time and starts affecting not only the long-term but also the short-term drainage dynamics. This is most clearly seen for the limiting case of pure water ($\kappa = 0.384$) shown in Fig. 2 (b), with $\Delta t = 0.312$ and $L^* = 500$. As before, the blue dashed line corresponds to the model without electrically induced shear stress. Note that the value of $t^* = 50$ s is significantly smaller than in Fig. 2 (a), but the difference between the predictions of the two models is al-

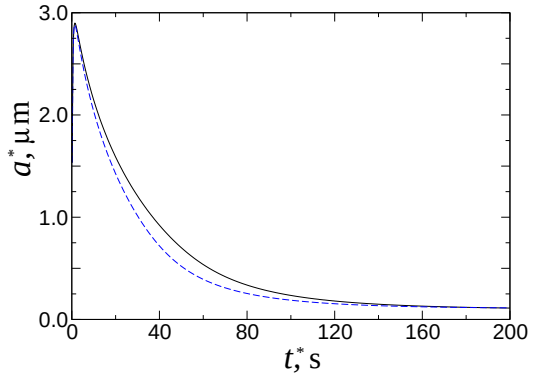

FIG. 3. (Color online) Film thickness at $r = 0$ as function of time for the same values as in Fig. 2 (bottom), with electrically induced shear stress included in the model (black solid line) and neglected (dashed blue line).

ready significant. In constrast, the difference at $t^* = 50$ s would be small for the parameter values corresponding to Fig. 2 (a).

Since the most significant changes of interface shape with time take place near the $r = 0$, evolution of the film thickness a^* at the axis of symmetry, illustrated in Fig. 3 for the pure water case, provides a useful insight into the overall dynamics of the interface. The range of values of time in the figure reflects the time scale of experimental observation. We do not attempt to resolve the details of the very fast initial dynamics since they are known to have little effect on experimentally relevant characteristics of drainage beyond $t^* \sim 1$ s. As before, the dashed line is used for the case when the shear stress contribution is neglected in the model. There is little difference in the predictions of the models during the first few seconds of drainage, but then the discrepancy becomes significant before eventually decreasing as the film flattens to take the equilibrium shape.

The results shown in Figures 2 and 3 clearly illustrate that using the correct shear stress balance is important not only from the standpoint of mathematical consistency of the asymptotic theory but also for answering practical questions, e.g. determination of the drainage rate over long periods of time. For all simulations we conducted, the previously overlooked effect of tangential electric field reduces the long-term drainage rates. This explains why imposing the no-slip condition instead of the Navier slip condition at the fluid interface resulted in better agreement with experiments in the study of Manica & Chan [12]: the no-slip at the interface reduces the outward drainage rate, i.e. has the same effect as the shear stress induced by the electric field. It is important to point out, though, that in reality the slow-down of the drainage process is most likely due to combination of the effects of partial immobilization by surfactants and the electrically induced shear stress. The relative importance of each can only be determined by accurately measuring and/or controlling both the surfactant concentration and the amount of electric charge at the deforming fluid interface.

The electrically induced shear stress is not due to variations of the surface tension but rather a result of direct action of the electric field on the charges present at the fluid interface. Based on equation (13), the relative importance of the shear stress contribution of the electric field as compared to the disjoining pressure term can be estimated as $\tilde{q}/(\kappa h \sinh \tilde{\psi})$. This implies that the tangential stress will always be significant for small values of κh, which is the ratio of the dimensional film thickness to the Debye length λ_D. This is exactly the condition of interest in many applications, i.e. the condition when there is a significant overlap of the electrical double layers of the two interfaces. When film thickness is much larger than the Debye length, the electrically induced tangential stress can be neglected, but then the significance of any electrostatic interaction of interfaces is small due to lack of sufficient overlap of the electrical double layers.

B. Comparison with previous studies

Let us now discuss comparison of the predictions of our model with the experimental data and previous numerical simulations of drainage. We start with the case of NaCl solution of concentration 0.25 mM. Figure 4 (top) shows the experimental measurements of film thickness at $t^* = 200$ s. at several locations, obtained by Hewitt et al. [2], together with numerical predictions based on different model formulations. The black solid line corresponding to the numerical solution of equation (13) and is in reasonably good agreement with the experimental data. The dashed blue line is obtained from the same equation but with the electrically induced contribution to the shear stress balance set to zero, clearly leading to underprediction of the values of film thickness. As discussed above, Manica & Chan [12] also observed in their numerical studies of drainage that the use of the standard zero shear stress condition at the fluid interface leads to smaller values of thickness than measured in experiments. To achieve better comparison with the experimental data, they proposed application of the no-slip condition at the deforming interface, motivated by the experimentally observed effect of interface immobilization by surfactants [13]. Applying the same approach in the framework of our model results in improved comparison with the experimental data, as illustrated by the dot-dashed line in Fig. 4 (top). (Note that our result is not identical to [12] due to minor differences in the model formulation, but is in fact very close). With the limited amount of experimental data in Fig. 4 (top), it is difficult to conclusively state which model provides better agreement with experiment, but since most experimental points fall between the solid and dot-dashed curves, it would be reasonable to conclude that a combination of partial immobilization of the interface and electrically

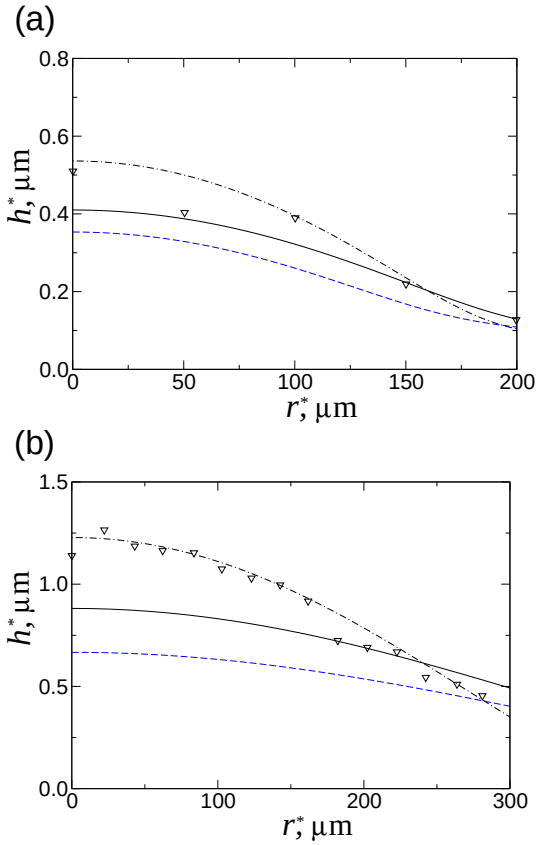

FIG. 4. (Color online) Experimental data (triangles) and predicted interface shapes from the numerical solution of equation (13) (solid lines) for (a) NaCl solution, $\kappa = 4.29$, $\hat{\psi} = -5.06$, $\Delta t = 0.221$, at $t^* = 200$ s; (b) pure water, $\kappa = 0.384$, $\hat{\psi} = -5.76$, $\Delta t = 0.3133$, at $t^* = 50$ s. Predictions of models neglecting the electrically induced shear stress are shown by dashed lines (with perfect slip at the deforming interface) and dot-dashed lines (with the no-slip condition at the deforming interface).

induced shear stress governs the dynamics of drainage.

Numerical results for the important special case of pure water have been discussed in the previous subsection. Comparison of the numerical interface shapes and the corresponding experimental data of Hewitt et al. [2] for this case is illustrated in Fig. 4 (bottom) using the same conventions for the three curves illustrating three different modeling approaches as in Fig. 4 (top). Once again, we observe that the solution of equation (13) with the zero shear stress at the liquid-gas interface is not providing a good fit to the experimental measurements. However, in contrast to Fig. 4 (top), addition of the electrostatic contribution to the shear stress results only in minor improvement of comparison with experiments. Taking into account the effect of immobilization, on the other hand, leads to a good fit to the experimental interface profile, in agreement with the observations of Manica & Chan [12]. Thus, we conclude that in pure water ex-

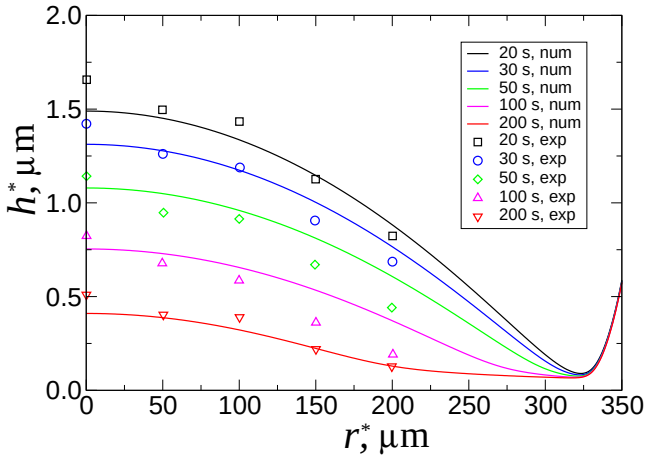

FIG. 5. (Color online) Time-dependent interface shapes for $\kappa = 4.29$, $\hat{\psi} = -5.06$, predicted by our model and compared with the experimental data of [2].

periment, the role of surfactant-induced immobilization is likely to be more significant than in the NaCl experiment. More studies are clearly needed to fully understand the relative importance of surfactant-induced immobilization effects and electrically induced tangential force at the interface over a range of concentrations.

All previous comparisons in the present section are based on interface snapshots at specific times. However, the experimental study of Hewitt et al. [2] provides data on the interface shapes at several different times, so to verify agreement with experiments for the NaCl solution it is important to check that data at all these times actually matches our model predictions. This is indeed the case, as illustrated in Fig. 5, clearly showing reasonable agreement for all experimentally studied times, from 20 s to 200 s. The comparison does involve a fitting parameter, which is the time of the initial downward shift of the capillary tube, but the same type of fitting procedure was employed by Manica & Chan [12].

C. Debye-Hückel approximation

Numerous studies of thin liquid layers take advantage of approximate expressions for disjoining pressure. It is natural to ask if approximate models can help better understand the physical effect introduced in the present work and define the conditions under which it is important. Even though not directly applicable to the experimental studies discussed above, the so-called Debye-Hückel approximation is a valuable tool for providing simple analytical formulas for electrostatic disjoining pressure when all the scaled potentials are small. Let us take advantage of this approximation to investigate the electrically induced shear stress. First, we note that the solution of the equation (10) at small ψ leads to the

following formula for the interfacial potential $\tilde{\psi}$,

$$\tilde{\psi} = \frac{\tilde{q}\sinh(\kappa h) + \hat{\psi}}{\cosh(\kappa h)}. \tag{15}$$

Interface shapes at small values of the potential, obtained using this approximation for $\tilde{\psi}$, are shown in Fig. 6 (top). Dashed line shows the solution with interfacial shear stress set to zero. We note that not only quantitative but also qualitative changes in the evolving interface shapes are apparent. The solution without the electrically induced shear stress is nearly flat everywhere except a small region near the minimum of the film thickness, while the actual interface shapes are nearly parabolic. In order to better understand the spatial variation of the tangential stresses, we plot the interfacial electric potential $\tilde{\psi}$ as a function of radial variable in Fig. 6 (bottom). The potential is nearly constant in the region of $r < 25$, but then changes rapidly near the point of minimum of thickness, going through two points of maximum. The availability of the simple analytical formula (15) makes it easy to interpret this result: the points of maximum of the potential are the zeros of ψ_h, reached at

$$h = \kappa^{-1}\cosh^{-1}\left[\hat{\psi}/(\kappa\tilde{q})\right],$$

which corresponds to two different values of r. We note that the potential variation with r near the left maximum is highly nonsymmetric, explaining why there is the net effect of reduction of the drainage rate.

The electrical charge density at the liquid-gas interface is determined by a combination of factors such as local charge regulation, interface stretching, and charge transport by the flow. In the present work, we avoid the complications of describing these factors and simply assume the charge density to be constant. However, this assumption may be violated when the transport of the interfacial charges by flow becomes significant enough to result in charge re-distrubution. In order to analyze this effect, we considered a modification of our model, in the framework of the Debye-Hückel approximation, by coupling the interface evolution to the equation for charge transport,

$$\tilde{q}_t + r^{-1}\left(r\tilde{u}\tilde{q}\right)_r = 0, \tag{16}$$

where the charge density is no longer assumed constant and is in fact found from the numerical solution, $\tilde{u}$ is the flow velocity at the interface. We start the simulations with the initial conditions correponding to the end of the initial rapid transient period and compare interface shapes predicted with fixed $\tilde{q} = -0.5$ and the charge density evolving simultaneously according to Eq. (16). Figure 7 illustrates the predictions of the two models at $t = 10$. Clearly, the model incorporating interfacial charge transport leads to even slower drainage rates that the constant-charge density model. A possible explanation of this fact is that local reduction of the interfacial charge density near the point of minimum film thickness leads to reduction of the local film thickness there and thus decrease of the flow rate through that cross-section.

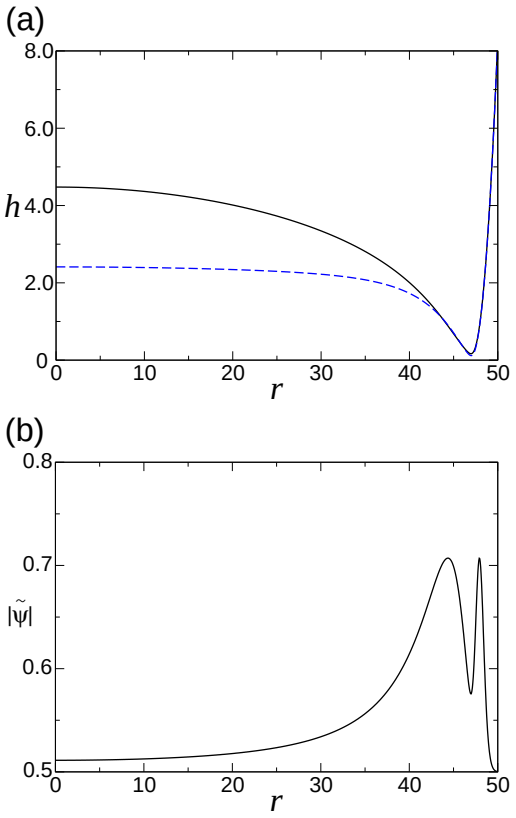

FIG. 6. (Color online) (a) Fluid interface shapes for $\hat{\psi} = -0.5$, $\tilde{q} = -0.5$, $\kappa = 1$, $t = 10^4$ obtained with the shear stress variations included into the model (black solid line) and neglected (blue dashed line); (b) The absolute value of the interfacial electrostatic potential plotted versus the radial coordinate at the same parameter values.

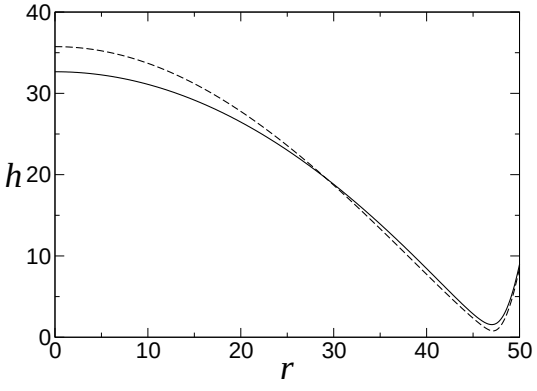

FIG. 7. Comparison of predicted interface shapes with and without charge transport for $\hat{\psi} = -0.5$, $\kappa = 1$, with fixed $\tilde{q} = -0.5$ (solid line) and $\tilde{q}$ found from the numerical solution of (16) (dashed line).

IV. CONCLUSIONS

We developed a mathematical model of drainage of the thin aqueous film formed when a gas bubble is pressed against a solid wall. The model describes lubrication-type viscous flow in the film coupled to the electrostatic interaction of electrical double layers formed near the solid-liquid and liquid-gas interfaces. In contrast to previous studies of drainage of water and aqueous solutions, we incorporate the effect of the electric field on the shear stress balance at the gas-liquid interface and show that this effect plays a significant role in the dynamics of drainage under a wide range of conditions, leading to slower drainage rates than can be expected by using the zero shear stress condition at the deforming interface.

Detailed comparisons of our model with experimental data are carried out, showing good agreement of predicted interface shapes with the experimental data on drainage of typical NaCl solutions. However, the agreement is rather poor for the case of pure water, indicating that a different effect, not related to electrically induced shear stress, is dominating the dynamics. We believe that this effect is most likely due to immobilization of the interface by surfactants, as suggested in the well-known numerical study of drainage by Manica and Chan [12]. We verified that excellent agreement with experiments can be obtained if the interface immobilization is accounted for.

While most of the results are based on the numerical solution of the nonlinear Poisson-Bolztmann equation for the electric potential, the limiting case of small potentials is also considered, leading to the Debye-Hückel approximation. Both interface shapes and variations of the interfacial electric potential are studied in the framework of this approximation. Also, the contributions due to transport of interfacial charges by the flow are analyzed and shown to result in even slower drainage rates than the models based on the constant fluid interface charge approximation.

V. ACKNOWLEDGEMENTS

This work was supported by the National Science Foundation, USA (grant No. CBET 0854318), and the National Research Tomsk Polytechnic University, Russia (grant No. VIU_ENIN_94_2014). We thank Dr. R. Manica for providing the files of experimental data used in our figures and the anonymous referees for a number of useful suggestions.

[1] L. R. Fisher, E. E. Mitchell, D. Hewitt, J. Ralston, and J. Wolfe, Colloids Surf. **52**, 163 (1991).
[2] D. Hewitt, D. Fornasiero, J. Ralston, and L. R. Fisher, J. Chem. Soc. Faraday Trans. **89** (1993).
[3] R. A. Pushkarova and R. G. Horn, Colloids Surfaces A **261**, 147 (2005).
[4] R. A. Pushkarova and R. G. Horn, Langmuir **24**, 8726 (2008).
[5] L. Y. Clasohm, J. N. Connor, O. I. Vinogradova, and R. G. Horn, Langmuir **21**, 8243 (2005).
[6] V. S. Ajaev, R. Tsekov, and O. I. Vinogradova, Phys. Fluids **19**, 061702 (2007).
[7] C. Y. Lin and J. C. Slattery, AIChE J. **28**, 147 (1982).
[8] R. Manica, J. N. Connor, R. R. Dagastine, S. L. Carnie, R. G. Horn, and D. Y. C. Chan, Phys. Fluids **20**, 032101 (2008).
[9] B. V. Derjaguin, N. V. Churaev, and V. M. Muller, *Surface Forces* (Plenum Press, NY, 1987).
[10] J. N. Israelachvili, *Intermolecular and Surface Forces* (Academic Press, London, 1992).
[11] R. Manica, J. N. Connor, , S. L. Carnie, R. G. Horn, and D. Y. C. Chan, Langmuir **23**, 626 (2007).
[12] R. Manica and D. Y. C. Chan, Phys. Chem. Chem. Phys. **13**, 1434 (2011).
[13] O. Manor, I. Vakarelski, X. Tang, S. O'Shea, G. Stevens, F. Grieser, R. R. Dagastine, and D. Y. C. Chan, Phys. Rev. Lett. **101**, 024501 (2008).
[14] D. Saville, Annu. Rev. Fluid Mech. **29**, 27 (1997).
[15] A. Oron, S. H. Davis, and S. G. Bankoff, Rev. Mod. Phys. **69**, 931 (1997).
[16] R. V. Craster and O. K. Matar, Rev. Mod. Phys. **81**, 1131 (2009).
[17] V. S. Ajaev, *Interfacial Fluid Mechanics: A Mathematical Modeling Approach* (Springer, New York, 2012).